Dynamics in the fundamental solution of a nonconvex conservation law

Yong-Jung Kim and Young-Ran Lee
Department of Mathematical Sciences, KAIST, 291 Daehak-ro,
Yuseong-gu, Daejeon 305-701, Korea, E-mail: yongkim@kaist.edu
Department of Mathematics, Sogang University, 5 Baekbeom-ro,
Mapo-gu, Seoul 121-742, Korea, E-mail: younglee@sogang.ac.kr

There is a huge jump in the theory of conservation laws if the convexity assumption is dropped. In this paper we study a scalar conservation law without the convexity assumption by monitoring the dynamics in the fundamental solution. Three extra shock types are introduced other than the usual genuine shock, which are left, right and double sided contacts. There are three kinds of phenomena of these shocks, which are called branching, merging and transforming. All of these shocks and phenomena can be observed if the flux function has two inflection points. A comprehensive picture of a global dynamics of a nonconvex flux is discussed in terms of characteristic maps and dynamical convex-concave envelopes.

1. Introduction

We consider the solution of a scalar conservation law,

$$\partial_t u + \partial_x f(u) = 0, \qquad x \in \mathbf{R},\ t > 0. \tag{1.1}$$

The goal of this paper is to understand the dynamics of shock and rarefaction waves when the flux function f is not convex. We assumes two hypotheses:

$$f \text{ has a finite number of inflection points,}$$
$$\frac{f(u)}{u} \to \infty \quad \text{as} \quad u \to \infty. \tag{1.2}$$

For a simpler presentation, we also assume $f \in C^1$ and, without loss of generality,

$$f(0) = f'(0) = 0. \tag{1.3}$$

We will focus on the dynamics of the fundamental solution, denoted by ρ, which is a nonnegative entropy solution that satisfies

$$\lim_{t \to 0} \rho(x,t) = \delta(x). \tag{1.4}$$

This signed fundamental solution has been constructed in [13] using its relation to convex-concave envelopes. We will classify the components of the fundamental solution and obtain the global dynamics of a nonconvex conservation law by combining them.

Nonlinear scalar conservation laws provide a shock wave theory in a simplest form, which is well understood for a genuinely nonlinear case (see [8, 19, 20, 24]). In particular, the Lax-Hopf transformation [20] may make the solution even explicit. This simplicity is from the fact that the information is only destroyed along a shock wave, but never produced. However, such a simplicity cannot be expected for nonconvex case and it is a completely different game without the convexity assumption. First of all, a nonconvex conservation law generates new types of shocks and some of them may produce new information. Furthermore, these shocks interact each other via branching, merging or transforming phenomena. These various phenomena show the essence for conservation laws one may obtain when the convexity assumption is dropped.

There are various examples of nonconvex flux which are from Buckley-Leverett equation, thin film equation, systems of conservation laws and many others (see [2, 3, 11, 27]). The existence and the uniqueness of a bounded solution and the convergence of zero viscosity limit hold true for both convex and nonconvex cases (see [1, 5, 19, 25]). The solution structure has been studied for a case with a single inflection point (see [1, 9]), which shows the complexity of the solution even with a single inflection point. The idea of this paper is to focus only on the fundamental solution, which allows us to glimpse the dynamics of a conservation law with a nonconvex flux function. The BV-boundedness of a solution holds for a uniformly convex case, but not for a general nonconvex one (see [6, 7, 9, 22, 26] for more regularity properties). We will see that the difference in the dynamics of the two cases is more drastic than the regularity theory.

The rest of this paper is organized as follows. In Section 2 a structural lemma, Lemma 2.3, is introduced, which gives basic relations between convex-concave envelopes and the evolution of the fundamental solution. It is this lemma that provides us a tool to closely monitor the dynamics of the fundamental solution. In Section 3, four types of shock waves are classified, which are left contact, right contact, double contact and genuine shock. These shocks can be increasing or decreasing ones depending on the flux function. Remember that only a decreasing genuine shock is allowed for a convex flux case. Three kinds of shock interactions are introduced in Section 4. Branching is a phenomenon that a single shock is divided into two smaller shocks and merging is a one that two shocks are combined into a single shock of a smaller size. If the flux changes its sign as in (4.1), a genuine shock can become a left or right contact. We call this phenomenon transforming.

In Section 5, rarefaction waves are discussed. For a convex flux case, a fundamental solution may have only a centered wave fan placed at the origin $(x, t) = (0, 0)$. However, for a nonconvex flux case, the centered rarefaction wave fan can be placed at any place. Furthermore, there exists another kind of rarefaction wave which is called a contact rarefaction. In Section 6, we classify possible shocks and shock interactions when the number of inflection points is given. We will see that if the number of inflection points is two, then all possible shocks and phenomena can be observed. Finally, a comprehensive scenario of a fundamental solution is given in Section 7 for a flux function with four inflection points. An illustration of the whole characteristic map is given in Figure 11. One may observe such an evolution of the fundamental solution by numerical computations (see Figure 12). In this computation the flux in Figure 10 has been used.

The study of solution behavior beyond the fundamental solution is a wide open area if the convexity of the flux function is not assumed. For example, the Riemann solution is given by fixed convex or concave envelops and hence the phenomena such as branching, merging and transforming are not observed. Hence, we need more than the Riemann solver to explain a general solution behavior. Notice that the Buckley-Leverett type nonconvex flux functions do not satisfy $(1.2)_2$. However, the convex-concave envelops technique in this paper is still applicable. For more discussions with possible open problems and further directions to study nonconvex conservation laws are given in Section 8.

2. Structural lemma for fundamental solutions

Denote the speed of a shock that connects u_1 and u_2 by

$$\sigma(u_1, u_2) := \frac{f(u_1) - f(u_2)}{u_1 - u_2}.$$

Suppose that an entropy solution $u(x,t)$ has a discontinuity along a curve $x = s(t)$. The discontinuity curve of an entropy solution or the discontinuity itself is called a *shock* or a *shock curve*. Then, the curve satisfies the Rankine-Hugoniot condition,

$$s'(t) = \sigma(u_-(t), u_+(t)), \quad u_\pm(t) = \lim_{y \to s(t)\pm} u(y, t). \tag{2.1}$$

A characteristic line $x = \xi(t)$ that emanates from a point (x_0, t_0) satisfies

$$\xi'(t) = f'(u(\xi(t), t)), \quad \xi(t_0) = x_0, \quad t \in I. \tag{2.2}$$

If $I \subset [t_0, \infty)$, then the characteristic line $\xi(t)$ is called a forward one and, if $I \subset [0, t_0]$, then it is called a backward one.

The uniqueness of a signed fundamental solution has been shown by Liu and Pierre [23, Theorem 1.1] for a Lipschitz continuous flux φ such that $\varphi([0, \infty)) \subset [0, \infty)$ and $\varphi(0) = 0$. In the followings we first obtain a similar uniqueness theorem under (1.2).

Theorem 2.1 (Uniqueness of a signed fundamental solution). *Suppose that the flux function $f \in C^1(\mathbf{R})$ satisfies (1.2) and $m > 0$ is given. Then, there exists a unique nonnegative solution $\rho_m(x, t)$ that satisfies (1.1) and*

$$\lim_{t \to 0} \rho_m(x, t) = m\delta(x). \tag{2.3}$$

Proof. It is enough to show the uniqueness of a nonnegative solution for $m > 0$. The assumptions (1.2) and (1.3) imply that there exists $b > 0$ such that $f(u) \geq -bu$ for all $u \geq 0$. Let $\varphi(u) = f(u) + bu$. Then $\varphi(0) = 0$ and $\varphi(u) \geq 0$ for all $u \geq 0$. Therefore, there exists a unique nonnegative solution to

$$u_t + \varphi(u)_x = 0, \quad \lim_{t \to 0} u(x, t) = m\delta(x) \tag{2.4}$$

(see [23, Theorem 1.1]). Let u be the nonnegative solution and v be its translation given by $v(x, t) = u(x - bt, t) \geq 0$. Then,

$$v_t + \varphi(v)_x = u_t - bu_x + f(u)_x + bu_x = 0.$$

One can easily check that, if u is an entropy solution that satisfies the entropy and the Rankine-Hugoniot jump conditions, then v is one as well. Therefore, v is an entropy solution to (1.1). Let $\tilde{v}$ be another nonnegative solution and $\tilde{u}$ be given similarly by $\tilde{v}(x,t) = \tilde{u}(x - bt, t)$. Then, since a nonnegative solution to (2.4) is unique, $u(x,t) = \tilde{u}(x,t)$ and hence $v(x,t) = \tilde{v}(x,t)$. □

Now we show a scaling argument using this uniqueness theorem.

Lemma 2.2. *Let ρ_m be the unique nonnegative solution of mass $m > 0$. Then,*

$$\rho(x,t) = \rho_m(mx, mt), \quad x \in \mathbf{R}, \ t > 0. \tag{2.5}$$

Proof. Let $u(x,t) = \rho_m(mx, mt)$ with $m > 0$. Then

$$u_t = m\partial_t \rho_m(mx, mt), \quad u_x = m\partial_x \rho_m(mx, mt)$$

and hence

$$u_t + f'(u)u_x = m\partial_t \rho_m(mx, mt) + mf'(\rho_m(mx, mt))\partial_x \rho_m(mx, mt) = 0.$$

Therefor, $u(x,t)$ is a solution of the conservation law. Furthermore, since

$$\int_{\mathbf{R}} \phi(x)u(x,0)dx = \int_{\mathbf{R}} \phi(x)\rho_m(mx,0)dx = \int_{\mathbf{R}} \phi(y/m)\delta(y)dy = \phi(0)$$

for any test function $\phi(x)$, $u(x,t)$ is the fundamental solution, i.e., $u = \rho$. Therefore, the uniqueness of a signed solution gives the relation (2.5). □

In the construction of a signed fundamental solution, the maximum value $\bar{\rho}$ and the maximum point $\zeta(t)$, i.e.,

$$\bar{\rho}(t) := \sup_x \rho(x,t), \quad \max\{\rho(\zeta(t)-,t), \rho(\zeta(t)+,t)\} = \bar{\rho}(t),$$

are used as parameters and then decided implicitly. The convex and concave envelopes are respectively defined by

$$h(u;\bar{\rho}) := \sup_{\eta \in A(0,\bar{\rho})} \eta(u), \quad k(u;\bar{\rho}) := \inf_{\eta \in B(0,\bar{\rho})} \eta(u), \tag{2.6}$$

where

$$A(0,\bar{\rho}) := \{\eta : \eta''(u) \geq 0, \ \eta(u) \leq f(u) \ \text{ for } \ 0 < u < \bar{\rho}\}, \tag{2.7}$$

$$B(0,\bar{\rho}) := \{\eta : \eta''(u) \leq 0, \ \eta(u) \geq f(u) \ \text{ for } \ 0 < u < \bar{\rho}\}. \tag{2.8}$$

One can easily check that, for any fixed $\bar{\rho} > 0$, $h(u;\bar{\rho})$ and $k(u;\bar{\rho})$ are convex and concave functions on the interval $(0,\bar{\rho})$, respectively. Since we consider a flux with a finite number of inflection points, the domain $(0,\bar{\rho})$ can be divided into a finite number of subintervals so that envelopes are identical to the flux or a line on each subinterval.

Finally, the fundamental solution is given by the inverse relation of

$$\begin{cases} \bar{h}(\rho(x,t),t) & = x \ \text{ for } x < \zeta(t), \\ \bar{k}(\rho(x,t),t) & = x \ \text{ for } x > \zeta(t), \end{cases} \tag{2.9}$$

where $\bar{h}$ and $\bar{k}$ satisfy

$$\partial_t \bar{h}(u,t) = \partial_u h(u;\bar{\rho}(t))), \quad \partial_t \bar{k}(u,t) = \partial_u k(u;\bar{\rho}(t))) \tag{2.10}$$

(see [13, Section 4] for details). The structure of the fundamental solution is analyzed in the rest of the paper using the dynamics and the relations of the envelopes. The following lemma is a summary of the basic relations and dynamics. We will use this structural lemma in analyzing the components and dynamics of fundamental solutions.

Lemma 2.3 (structural lemma for fundamental solutions). *Let $0 = a_0 < a_1 < \cdots < a_{i_0} = \bar{\rho}(t)$ be the minimal partition of $[0, \bar{\rho}(t)]$ such that the convex envelope $h(u;\bar{\rho}(t))$ is either linear or identical to $f(u)$ on each subinterval (a_i, a_{i+1}), $0 \le i < i_0$. Similarly, let $0 = b_0 < b_1 < \cdots < b_{j_0} = \bar{\rho}(t)$ be the minimal partition related to the concave envelope $k(u;\bar{\rho}(t))$. Let $\zeta_0(t)$ is the maximum point in the sense that $\bar{\rho}(t) = \max(\rho(\zeta_0(t)+,t), \rho(\zeta_0(t)-,t))$ and $\mathrm{spt}(\rho(\cdot,t)) = [\zeta_-(t), \zeta_+(t)]$.*
  (i) The linear parts of the envelopes are tangent to the flux, i.e.,

$$h'(a_i;\bar{\rho}(t)) = f'(a_i), \qquad i = 1, \cdots, i_0 - 1,$$
$$k'(b_j;\bar{\rho}(t)) = f'(b_j), \qquad j = 1, \cdots, j_0 - 1.$$

  (ii) The maximum $\bar{\rho}(t)$ is strictly decreasing as $t \to \infty$.
  (iii) The solution $\rho(x,t)$ increases in x on the interval $(\zeta_-(t), \zeta_0(t))$. If $h(u;\bar{\rho}(t))$ is linear on (a_i, a_{i+1}), $\rho(x,t)$ has an increasing discontinuity that connects $u_- = a_i$ and $u_+ = a_{i+1}$. If $f(u) = h(u;\bar{\rho}(t))$ on (a_i, a_{i+1}), $\rho(x,t)$ has a rarefaction profile that continuously increases from $u = a_i$ to $u = a_{i+1}$.
  (iv) The solution $\rho(x,t)$ decreases in x on the interval $(\zeta_0(t), \zeta_+(t))$. If $k(u;\bar{\rho}(t))$ is linear on (b_j, b_{j+1}), $\rho(x,t)$ has a decreasing discontinuity that connects $u_- = b_{j+1}$ and $u_+ = b_j$. If $f(u) = k(u;\bar{\rho}(t))$ on (b_j, b_{j+1}), $\rho(x,t)$ has a rarefaction profile that continuously decreases from $u = b_{j+1}$ to $u = b_j$.

Lemma 2.3 gives the dynamics of the fundamental solution in terms of convex-concave envelopes. First, the number of discontinuities and their left and right hand limits are given by the convex-concave envelopes if the maximum $\bar{\rho}(t)$ at a specific time $t > 0$ is known. However, we do not know the location of a discontinuity. The discontinuities are connected by rarefaction waves. However, if the flux is not convex, the structure of rarefaction waves are quite complicated and are not functions of x/t (see Section 5).

In Figure 1(a), convex-concave envelopes on a given domain $[0, \bar{\rho}(t)]$ are illustrated. Note that, the graph of the flux $f(u)$ is tangent to the u-axis at the origin since (1.3) is assumed. The minimal partition values a_i's for the convex envelope are marked at the corresponding tangent points. Two linear parts of the convex envelope indicate that the fundamental solution have two increasing discontinuities. One of them jumps from 0 to a_1 and the other from a_2 to a_3. These discontinuities satisfy the entropy condition. Similarly the concave envelope and the corresponding minimal partition b_j's provide the decreasing shocks.

As the maximum $\bar{\rho}(t)$ decreases, the corresponding envelopes evolve continuously. However, if the end point $(\bar{\rho}(t), f(\bar{\rho}(t)))$ reaches to a tangent point, then
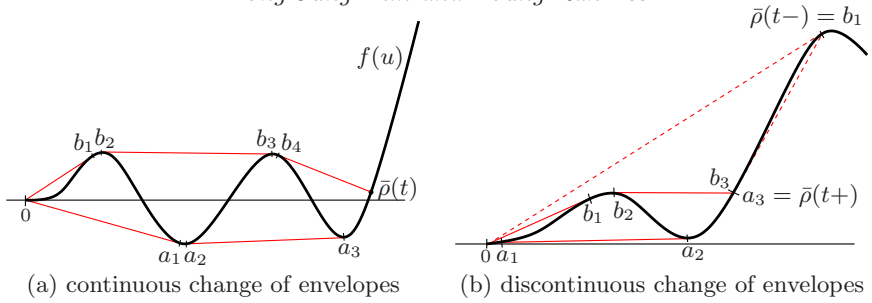
(a) continuous change of envelopes   (b) discontinuous change of envelopes

Figure 1. Examples of envelopes and minimal partitions. consist of 0, $\bar{\rho}(t)$ and coordinates of the horizontal axis (or u-axis) of the tangent points. If both of the envelopes meet with linear parts as in (b), then the maximum jumps to the nearest interior partition point a_3 in the figure.

the envelopes change discontinuously and an example is given in Figure 1(b). The envelopes in dashed lines are the case when $\bar{\rho}(t-) = b_1$. This implies that the maximum value $\bar{\rho}(t-)$ is connected to the value a_3 by an increasing shock and also connected to 0 by a decreasing shock. In other words the solution has an isolated singularity. The case $a_3 < \bar{\rho} < b_1$ is not admissible by the same reason. Therefore $\bar{\rho}$ jumps from b_1 to a_3 and the envelopes jump from the dashed ones to the solid ones in the figure. In particular the minimal partition for the concave envelope has new members and should be re-indexed as in the figure.

3. Classification of shocks

The dynamics of shocks is the key in understanding the structure of a fundamental solution of a conservation law. In this section we classify the types of shocks. Let $x = s(t)$ be a shock curve of $\rho(x,t)$ and $u_0^\pm = \lim_{\varepsilon \downarrow 0} \rho(s(t_0) \pm \varepsilon, t_0)$ be one-sided limits[1]. Let $x = \xi_+(t)$ be the maximal characteristic curve and $x = \xi_-(t)$ be the minimal one, where both of them emanate from the given point $(s(t_0), t_0)$. Then, the backward and the forward characteristic curves satisfy

$$\xi'_+(t_0) = f'(u_0^+), \quad \xi'_-(t_0) = f'(u_0^-), \tag{3.1}$$

where the derivatives of characteristic curve are understood as one sided ones depending on its domain. We are interested in the characteristic curve that satisfies (3.1) since they are the ones that carry the information.

One may obtain the following well known relations from the Oleinik entropy condition,

$$f'(u_0^-) \geq s'(t_0) \geq f'(u_0^+). \tag{3.2}$$

In the followings we classify the shocks into four types.

3.1. Genuine shock

If both inequalities in (3.2) are strict, i.e.,

$$f'(u_0^-) > s'(t_0) > f'(u_0^+), \tag{3.3}$$

---

[1]In this notation the subindex, $_0$, indicates the time t_0 and the super indexes, $^\pm$, indicate right and left side limits. Since ρ may have multiple discontinuities, $u_0^\pm$ is used instead of $\rho_0^\pm$.

then the shock curve $x = s(t)$ is called a *genuine shock* and denoted by the letter 'G' in figures. If a faster characteristic line $x = \xi_-(t)$ collides to the slower shock curve $x = s(t)$ from the left at time $t = t_0$, it should come from the past (or as $t \to t_0-$). Similarly, if the slower characteristic line $x = \xi_+(t)$ collides to the shock curve from the right, then it should also come from the past. Therefore, for a genuine shock case, characteristics satisfying (3.1) are backward ones and

$$\xi'_-(t) > s'(t) > \xi'_+(t), \quad t_0 - \varepsilon < t < t_0 \tag{3.4}$$

for some $\varepsilon > 0$. If one may take the domain as $0 < t < t_0$, then the characteristic curve is called global, which is always the case with a convex flux. However, if the flux is nonconvex, the characteristic curves are not necessarily global.

Proposition 3.1. *A signed fundamental solution has at most one genuine shock, and it has one if and only if the convex or the concave envelope is a non-horizontal line. Furthermore, the genuine shock always connects the maximum to zero.*

Proof. Suppose that a shock connects a value of an intermediate partition point, say a_i with $0 \neq i \neq i_0$. Since the shock speed $s'(t)$ is given by the relation in (2.1), Lemma 2.3(i) gives that

$$s'(t) = h'(a_i; \bar{\rho}(t)) = f'(a_i) = \xi'(t), \quad t_0 - \varepsilon < t < t_0.$$

Therefore, at least one of the inequalities in (3.2) is an equality and hence the shock is not a genuine one. If a genuine shock connects the zero and the maximum, the corresponding envelope should be a line. Furthermore, since both envelopes can not be lines at the same time, a fundamental solution has at most one genuine shock at any given time.

$\square$

If the convex or concave envelope is a horizontal line, then due to the normalization (1.3), one of the inequalities in (3.2) is an equality. This is a transition stage of a genuine shock into a contact discontinuity which will be discussed in Section 4. Now suppose that a concave envelope is a non-horizontal line. Of course, the discontinuity connects the zero value and the maximum. We may easily see that if the line is not tangent to the graph of the flux, then it gives a genuine shock. Suppose that the line is tangent to the flux at the maximum as in Figure 1(b). Then the flux is locally concave near the maximum value $u = \bar{\rho}(t)$ and hence the convex envelope is also linear at the point $(\bar{\rho}(t), f(\bar{\rho}(t)))$. This implies that the maximum is an isolated singularity which is not admissible. Therefore, such envelopes do not exist. The same arguments are applied to the convex envelope.

If the flux is convex, its concave envelope is simply a non-horizontal line and gives a decreasing genuine shock all the time. Furthermore, there are no other types of shocks for the convex flux. Figure 2(a) is an illustration of a genuine shock.

3.2. Contact shocks

A shock is called a *contact* if it is not a genuine shock. If both inequalities in (3.2) are equalities, i.e.,

$$f'(u_0^-) = s'(t_0) = f'(u_0^+), \tag{3.5}$$

(a) genuine shock   (b) double contact   (c) left contact   (d) right contact
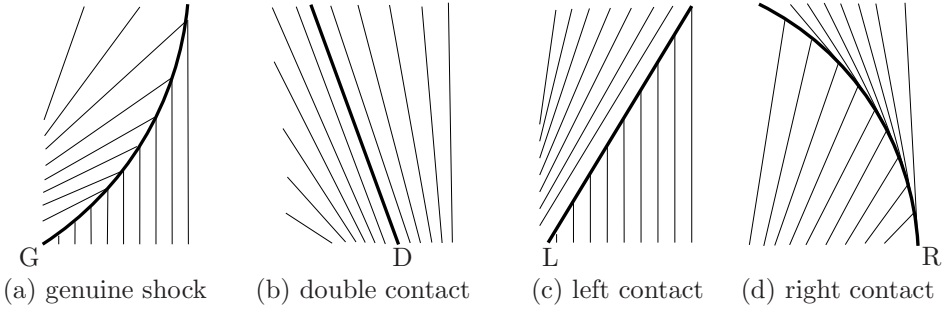
Figure 2. [xt-plane] Shocks of a nonconvex scalar conservation law are classified into four types.

then the shock is called a *double sided contact* or simply *double contact* and denoted by 'D' in figures. One can easily find such a discontinuity from convex-concave envelopes. Let a_i, $i = 0, \cdots, i_0$, be the minimal partition in Lemma 2.3 related to the convex envelope h. One can easily see that if h is linear in an interior subinterval (a_i, a_{i+1}) (i.e., $a_i \neq 0$ and $a_{i+1} \neq \bar{\rho}(t)$), then Lemma 2.3($i$) implies that (3.5) is satisfied. In this case the shock is placed between two rarefaction waves. Since the shock speed is constant until the tangent point a_{i+1} stays in the minimal partition, the double sided contact is a line parallel to adjacent characteristic lines (see Figure 2(b)). One may similarly consider double sided contacts related to the concave envelope.

If one of the inequalities in (3.2) is an equality and the other one is a strict inequality, then we call it a *single sided contact*. If

$$f'(u_0^-) = s'(t_0) > f'(u_0^+), \tag{3.6}$$

then this single sided contact is called a *left sided contact* or simply *left contact* and denoted by 'L' in figures. This means that the characteristic lines on the left hand side of the shock curve have the same speed as the one of the shock. Hence the characteristic lines are tangent to the shock curve from the left hand side (see Figures 2(c)).

Similarly, if

$$f'(u_0^-) > s'(t_0) = f'(u_0^+), \tag{3.7}$$

then this single sided contact is called a *right sided* or *right contact* and denoted by 'R' in figures.

Proposition 3.2. *A signed fundamental solution has two or three single sided contacts counting a genuine shock as two. If there is no genuine shock at a moment, then there exist at least one right and left contacts for each.*

Proof. A single sided contact should connect the maximum $\bar{\rho}(t)$ or the zero value to an interior partition value. If a discontinuity connects two interior partition points, then it is a double sided contact as discussed before. Since the maximum can not be connected by two shocks (see the comments following Figure 1(b)), the total number of contact shocks is at most three.   □

Proposition 3.3. *Double sided contacts are lines. Single sided contacts connected to zero are lines. There exists exactly one shock connected to the maximum $\bar{\rho}(t)$, which is the only one that moves with a nonconstant speed.*

Proof. We have already observed that the double sided contacts are lines. Single sided contacts connected to the zero value are also lines by the same reason that the linear part of the corresponding envelope is not changed as long as the contact is a single sided one. For example, consider a right contact case. Then, since 0 is the minimum, the contact is an increasing shock and hence the convex envelope is considered. Since the shock speed $s'(t)$ is given by the relation in (2.1), Lemma 2.3(i) gives that

$$s'(t) = h'(a_1; \bar{\rho}(t)) = f'(a_1),$$

where a_1 is the first interior partition point, which is constant as long as the right contact remains as it is. Hence, the right contact is a line. The left contact case is similar (see Figure 2(c)).

Now consider a left contact that connects the maximum $\bar{\rho}(t)$. Then, it is an increasing shock that connects the maximum to the last interior partition point a_{i_0-1}. Hence the shock speed is

$$s'(t) = h'(a_{i_0-1}; \bar{\rho}(t)) = f'(a_{i_0-1}),$$

Since the maximum of the fundamental solution $\bar{\rho}(t)$ strictly decreasing, the slope of the convex envelope at the maximum point is strictly increasing. Hence the left contact is not a line, but is curved to right since the propagation speed is increasing. One can show the similar behavior for the right contacts and the difference is that the right contact is curved to left (see Figure 2(d)). The genuine shock is similar as the contacts that connects to the maximum value $\bar{\rho}(t)$. □

According to the previous propositions, there exists only one shock that connects the maximum $\bar{\rho}(t)$. This shock is a genuine shock or a single sided contact that moves along a curve. All the other shocks propagate with a constant speed. Hence, all the dynamics of shock waves are produced along the shock that connects the maximum $\bar{\rho}(t)$ which is the only curved one of the signed fundamental solution. Furthermore, if this shock is a single sided contact, it produces new information.

Remark 3.4 (Information generating contact shock). *Consider the linear part of the concave envelope in Figure 1(a) that connects the maximum and an interior partition value b_4. First, note that the right hand side limit of the shock is b_4 since the concave envelope gives a decreasing shock. The speed of the characteristic line carrying this value is $f'(b_4)$ which is identical to the shock speed and hence the corresponding discontinuity is always a right contact. One can easily see that the slope of the linear part decreases as $\bar{\rho}(t)$ decreases (i.e., as t increases). Therefore the shock curve makes a turn to the left hand side as t increases like in Figure 2(d). Furthermore, the interior tangent value b_4 increases, which indicates that the range covered by rarefaction wave is increasing. In other words new information is produced and propagates to the future. Therefore, the characteristic line $x = \xi_+(t)$ touching the shock from the right hand side has a domain $t \in (t_0, t_0 + \varepsilon)$ for some $\varepsilon > 0$. In Figure 2(d) this kind of right contact has been illustrated. Even though*

the previous discussions are in terms of the concave envelope, one may repeat them with the convex envelope and obtain the dual statements.

4. Dynamics of shocks

The convex-concave envelopes have one end at the origin and the other end at the maximum point $(\bar{\rho}(t), f(\bar{\rho}(t)))$ with $\bar{\rho}(t) = \sup_x \rho(x, t)$. Since the maximum $\bar{\rho}(t)$ decreases in time t, the envelopes and the corresponding minimal partitions change. In the followings we consider the dynamics of shock curves by tracking these changes.

4.1. Branching

A shock curve may split into two smaller shocks divided by a rarefaction wave and we call this phenomenon *branching*. Consider a shock curve that connects the maximum value $\bar{\rho}(t)$. Then it should be a genuine shock or a single sided contact. If the corresponding linear part of the envelope touches a hump of the graph of the flux $f(u)$ on its way (see Figures 10(b) and 10(c)), it will split into two linear parts with a convex or a concave part in between. Since both of these two linear parts belong to the convex envelope or concave envelope, both shocks are increasing ones or decreasing ones. In other words an increasing shock splits into two smaller increasing shocks and a decreasing one into two smaller decreasing ones.

One can easily see that, at the moment the branching process starts, the linear parts of the envelope corresponding to the incoming and outgoing shocks are all the same line. Hence, the slopes of shock curves at the branching point in the xt-plane are identical and hence they form smooth curves of branching as in Figure 3.

Since the incoming shock is connected to the maximum $\bar{\rho}(t)$, one of the outgoing shocks connects the maximum, which should be a single sided contact. If the incoming shock is a single sided contact, then the other outgoing shock is a double sided contact as in Figure 3(a). Therefore, we may conclude that if the incoming shock is of single sided, it splits into one single sided and one double sided contacts. Similarly, if the incoming shock is a genuine shock, then it splits into two single sided contacts (see Figure 3(b)). Note that type D doesn't split. In summary, branching process is classified as the following.

Proposition 4.1. *There are three cases of branching classified by the incoming and outgoing shocks, which are (i) R→R+D, (ii) L→L+D, and (iii) G→R+L. Shock curves are smooth after a branching incident.*

4.2. Merging

Two shocks can be combined and then form a single shock. We call this phenomenon *merging*. In the process these two shocks have different monotonicity. One may see this phenomenon from the change of envelopes. As the maximum value $\bar{\rho}(t)$ decreases, two linear parts of convex and concave envelopes may meet at a point, say $(\bar{\rho}(t_0), f(\bar{\rho}(t_0)))$ (see Figures 1(b)). However, in this case it gives a removable jump (see [13, Lemma 3(iii)]) and the maximum of the fundamental solution has a decreasing jump from $\bar{\rho}(t_0+)$ to $\bar{\rho}(t_0-)$. In this case $\bar{\rho}(t_0-)$ is the largest interior partition point (e.g., the point a_3 in Figure 1(b)).
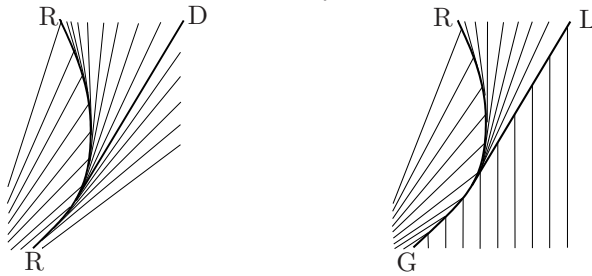
(a) branching (R→R+D)   (b) branching (G→R+L)

Figure 3. [xt-plane] There are three kinds of branching process. The third one is
'L→L+D'.

Remark 4.2 (Discontinuous change of envelopes)**.** *A sudden change of envelopes
after a merging incident gives several consequences (see Figure 1(b)). (i) The slopes
of the linear parts of the envelopes related the two incoming shocks and one outgoing
shock are all distinct and hence the shock curves are not differentiable after merging.
(ii) The new nonlinear part of the concave envelope gives a centered rarefaction
wave fan (see Section 5.1). (iii) The evolution of the fundamental solution is rather
independent of the values of the flux function on the interval $(\bar\rho(t_0+), \bar\rho(t_0-))$. For
example, even if one changes the values of the flux for $u \in (\bar\rho(t_0+), \bar\rho(t_0-))$ in Figure
1(b), the fundamental solution is not changed as long as its graph stays inside the
dashed lines. (Such a change of flux function makes a difference for general solutions
of course.)*
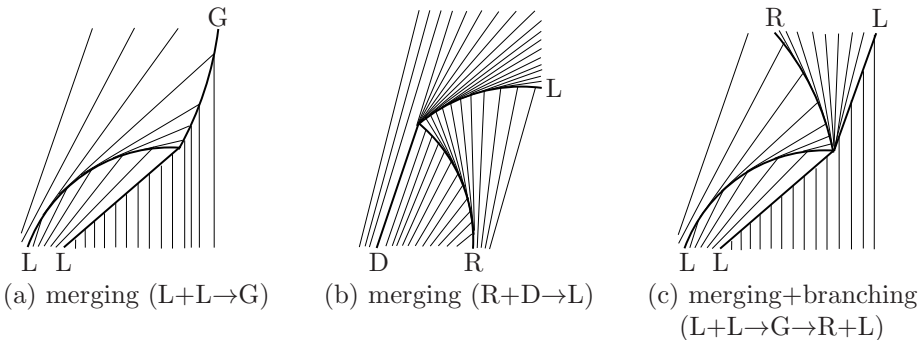
(a) merging (L+L→G)   (b) merging (R+D→L)   (c) merging+branching
                                                    (L+L→G→R+L)

Figure 4. [xt-plane] There are two kinds of merging. The last figure shows an example
when merging and branching occur simultaneously.

In Figure 4(a) two left contacts merge into a genuine shock. If a right contact is
merged with ap double sided contact, then a left contact is produced as in Figure
4(b). Note that merging is not exactly the reverse process of branching. In a merging
process, two shocks of different monotonicity produces a single smaller shock and
however, in a branching process, two shocks of the same monotonicity are produced.
Another difference is that the shock curve is not smooth after a merging process.
In summary, merging process is classified as the following.

Proposition 4.3. *There are four cases of merging classified by the incoming and outgoing shocks, which are (i) R+R→G, (ii) L+L→G, (iii) R+D→L, and (iv) L+D→R. The shock curves are not differentiable after a merging incident.*

4.3. Merging + Branching

Merging and branching are basic phenomena in the dynamics of discontinuities. These two phenomena may appear at the same time. Since the envelopes may change discontinuously after a merging process, a branching may follow immediately after it. Consider the example in Figure 1(b), where two incoming shocks meet at a point. Then, the merging process in the figure produces one left contact and one right contact, where the corresponding figure is in Figure 4(c). Notice that the outgoing shocks are of the same monotonicity. In this example they are given by the concave envelope and hence they are decreasing ones. It is also possible that there are more than two out going shocks. For example, if there are many wiggles in the inside hump of Figure 1(b), then there can be many outgoing shocks with same monotonicity with each other. However, all extra smaller contacts are double sided contacts for those cases. We finally obtain the following from Propositions 4.1 and 4.3.

Proposition 4.4. *There are four possible situations of 'branching after merging' classified by the incoming and outgoing shocks, which are (i) R+R→G→R+L, (ii) L+L→G→R+L, (iii) R+D→L→L+D, and (iv) L+D→R→R+D.*

4.4. Transforming

A shock may change its type without branching or merging and we call this phenomenon *transforming*. This phenomenon may appear only if

$$f\big([0,\infty)\big) \nsubseteq [0,\infty). \tag{4.1}$$

The only possible scenario is that a genuine shock is transformed to a single sided contact. It always happens when a genuine shock changes its direction from the negative one to the positive one or in the other way. For example consider a genuine shock that moves at a negative speed as in Figure 5(a). If it stops and then moves to the positive direction, then it is not a genuine shock any more. It becomes a left contact as one can see from the figure. Similarly, if a genuine shock changes its direction from the positive one to the negative one, then it becomes a right contact.

Proposition 4.5. *There are two kinds of transforming phenomena under (4.1), which are (i) G→R, (ii) G→L.*

4.5. Merging +Transforming

In Figure 4(a) two single sided contacts are merged into a genuine shock. If the transformation appears simultaneously, then one may see the phenomenon that two contacts of single sided are merged into a single sided contact as in Figure 5(b). One may consider this phenomenon as an example of merging. However, instead of placing it in the section for merging, we have separated the phenomenon in this section since the transforming process can be forgotten. Furthermore, the
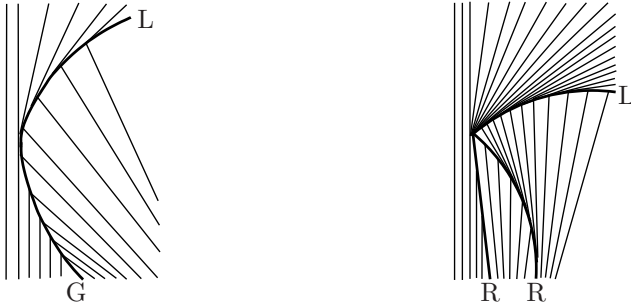
(a) transforming (G→L)   (b) merging+transforming (R+R→G→L)

Figure 5. [*xt*-plane] Transforming can be observed under an extra condition (4.1).

transformation phenomena can be found only under the extra hypothesis (4.1). Hence the phenomena in the following proposition do not appear if $f\big([0,\infty)\big) \subseteq [0,\infty)$.

Proposition 4.6. *There are two possible situations of 'transforming after merging' classified by the incoming and outgoing shocks if (4.1) holds, which are (i) R+R→G→L, (ii) L+L→G→R.*

Combining Propositions 4.3 and 4.5, there are two more possibilities of $R + R \to G \to R$ and $L + L \to G \to L$. However, these cases are not possible for the following reasons. First, the genuine shock obtained after a merging process of two right contacts moves to left since the right contact connecting to the zero value has negative speed under the assumptions $(1.2)_2$ and (1.3). Hence, it turns into a left contact after a transformation. Hence the possibility of $R + R \to G \to R$ is removed. Similarly, a phenomenon of $L + L \to G \to L$ is not possible, neither.

5. Structure of rarefaction waves

There is no contact shock for a convex flux case and hence all the characteristics of a fundamental solution carrying the information of a non-zero value are emanated from the origin. Therefore, if a fundamental solution ρ has a rarefaction profile at a point (x,t), the speed of the characteristic line that passes through the point is x/t and hence it should be satisfied that $f'(\rho(x,t)) = x/t$. Furthermore, since f' is invertible if the flux is strictly convex, the rarefaction wave should be given by the following relation

$$\rho(x,t) = g(x/t), \qquad a(t) \le x \le b(t), \tag{5.1}$$

where $f'(g(x)) = x$ and $[a(t), b(t)]$ is the support of the fundamental solution $\rho(\cdot, t)$. However, if the flux is not convex, then there may exist contact shocks and hence there are various possibilities for the starting point of the characteristic line. Furthermore, since f' is not invertible in the whole domain, one should clarify the correct profile that gives the rarefaction wave. In the followings we classify the rarefaction waves.

5.1. Centered rarefaction wave fans

There are two kinds of centered rarefaction waves. The first one is the one produced from the initial profile of the Dirac-measure and hence centered at the origin.

Let $h(u; \infty)$ be the convex envelope of the flux and $0 = a_0 < a_1 < \cdots < a_{i_0} < \infty$ be the minimal partition. Then the rarefaction wave is given as

$$\rho(x, t) = g_\infty(x/t), \qquad a(t) \le x \le b(t), \ 0 < t < \varepsilon, \tag{5.2}$$

where the similarity profile $g_\infty(x)$ is a piecewise continuous function that satisfies $h'(g_\infty(x); \infty) = x$. Notice that the function $g_\infty(x)$ may have a discontinuity and hence $\rho(x, t)$ given by (5.2) may have a discontinuity which is actually contact. Therefore, the rarefaction wave in (5.2) should be understood as a sequence of rarefaction waves divided by contacts. In Figure 11 an example of initial centered rarefaction wave can be found for $t > 0$ small. In the figure one may find the wave fan bounded by a genuine shock and a right contact. One may also find the inside profile is divided by a double sided contact.

A centered rarefaction wave may also appear after a merging process. If a shock collides to another one, then the envelopes change discontinuously and a centered rarefaction wave may emerge. For example consider the merging process in Figure 1(b) and let (x_0, t_0) be the merging point. Then the concave envelope jumps from the dashed one to the solid ones and a rarefaction part in the interval (b_2, b_3) is added to the concave envelope, Figure 1(b), which generates a centered rarefaction wave given as

$$\rho(x, t) = g_1 \left(\frac{x - x_0}{t - t_0} \right), \quad \xi(t) \le x \le s(t), \quad t_0 < t < t_0 + \varepsilon, \tag{5.3}$$

where g_1 is the inverse function of the flux on the domain (b_2, b_3) and the wave is bounded by a contact line of single sided and a characteristic line, which are given by

$$\xi(t) = x_0 + f'(b_2)(t - t_0), \ s(t) = x_0 + \frac{f(b_1)}{b_1}(t - t_0), \ t_0 < t < t + \varepsilon.$$

The wave fan which is between two outgoing contacts of single sided in Figure 4(c) and emanates from the branching point is a corresponding case.

One may also observe a centered rarefaction wave bounded by two characteristic lines. Consider the change of envelopes in Figure 10(d) after a merging. Then the interior partition point a_2 jumps from a_2^- to a_2^+ and a rarefaction part in the interval (a_2^-, a_2^+) is added to the convex envelope, which generates a centered rarefaction wave given by

$$\rho(x, t) = g_2 \left(\frac{x - x_0}{t - t_0} \right), \quad \xi_1(t) \le x \le \xi_2(t), \quad t_0 < t < t + \varepsilon, \tag{5.4}$$

where g_2 is the inverse function of the derivative of the convex envelope of the flux on the domain (a_2^-, a_2^+) and the wave fan is bounded by two characteristic lines, which are given by

$$\xi_1(t) = x_0 + f'(a_2^-)(t - t_0), \quad \xi_2(t) = x_0 + f'(a_2^+)(t - t_0), \quad t_0 < t < t + \varepsilon.$$

Remark 5.1. *The solution is continuous along the characteristic ξ_1, but not differentiable. This kind of regularity has been mentioned in Dafermos [9]. The rarefaction wave fan is bounded by a characteristic line at least one side. However, it is possible that there exist several contacts of type D inside of the fan.*

Proposition 5.2. *If a portion of the graph of the flux is added to the envelopes after a merging phenomenon, a centered rarefaction wave fan appears.*

5.2. Contact rarefaction

A centered rarefaction wave fan of a fundamental solution is produced instantly at the moment of the initial time or a merging phenomenon. On the other hand, a contact rarefaction wave is produced continuously along a single sided contact shock connected with the maximum value $\bar{\rho}(t)$. A typical example can be found in Figures 10(a) and 10(b). The concave envelope in Figures 10(a) shows that it is about the moment that the genuine shock splits into two contacts. The concave envelope at a later time is given in Figure 10(b), which shows that the rarefaction region (b_1, b_2) is expanding. This indicates that new informatio n is being produced and propagates to the future. On the other hand the rarefaction region $(a_3, \bar{\rho}(t))$ from the convex envelope is shrinking. In other words the information from the past is destroyed if it meets this shock.

In summary a contact rarefaction wave is produced by the single sided contact which connects the maximum from one side. For example, the right contact R in Figure 10(b) connecting b_2 and $\bar{\rho}(t)$ is the corresponding one. This single sided contact erases the information of the past from one side and produces new information from the other side.

6. Shock classifications on the number of inflection points

In this section we discuss what kinds of shock waves and their dynamics may or must appear in the evolution of the fundamental solution when the number of inflection points of the flux function is given. Note that we are taking the hypotheses (1.2) and (1.3) for simplicity and one may easily extend the theory without them. For example, one may consider the case with $\frac{f(u)}{u} \to -\infty$ as $u \to \infty$ instead of $(1.2)_2$ and obtain dual arguments in this section.

6.1. Convex flux function

Flux functions without any inflection point have been considered by many authors and are well understood. Such a flux is convex under the assumption $(1.2)_2$. In this case the fundamental solution has a simple structure

$$\rho(x, t) = \begin{cases} g\left(\frac{x}{t}\right), & 0 < x < b(t), \\ 0, & \text{otherwise,} \end{cases}$$

where $f'(g(x)) = x$ and $b(t)$ is given by the relation $\int_0^{b(t)} g\left(\frac{x}{t}\right) dx = 1$. The fundamental solution has a genuine shock at $x = b(t)$. A contact shock does not exist and hence the dynamics between shocks such as a merging, branching or transforming is never observed.

6.2. Flux function with a single inflection point

If the number of inflection points of the flux function is odd and $(1.2)_2$ and (1.3) are satisfied, then the flux function should be negative in a region $u \in (0, u_0)$ for

some $u_0 > 0$ and $f([0,\infty)) \nsubseteq [0,\infty)$. Therefore, if a flux function has a single inflection point, it should be as in Figure 6. In that case the fundamental solution should start with a genuine shock and a right sided contact. Then, the genuine shock is transformed to another right contact and the two right contacts are merged into a genuine shock. If $\frac{f(u)}{u} \to -\infty$ as $u \to \infty$ instead of $(1.2)_2$, then left sided contacts will appear in the place of right sided ones. However, a double sided contact and a branching phenomenon never appear.
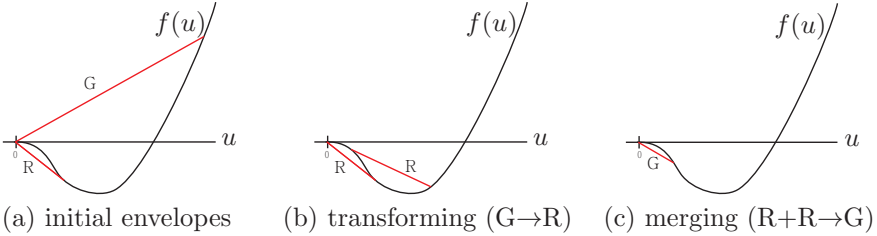

(a) initial envelopes   (b) transforming (G→R)   (c) merging (R+R→G)

Figure 6. Flux function with a single inflection point:

6.3. Flux function with two inflection points

If the number of infection points is a non-zero even number, we may split the case into two. First consider a case that $f([0,\infty)) \subseteq [0,\infty)$ as in Figure 7. It is clear that we cannot observe a transforming phenomenon in this case. However, we can observe all sorts of shocks and the other phenomena. As illustrated in Figure 7(a), the fundamental solution starts with a genuine shock and a double sided contact. Then, the genuine shock is split into a left and a right contacts and the right contact and the initial double sided contact are merged into a left contact. Finally the two left contacts are merged into a genuine shock which is the final stage of the dynamics.

Now we consider the other case that $f([0,\infty)) \nsubseteq [0,\infty)$ as in Figure 8. As illustrated in Figure 8(a), the fundamental solution starts with a genuine shock and a right sided contact. The initial genuine shock is split into a left and a right contacts and then the new right contact and the initial right contact are merged into a genuine shock. This genuine shock is transformed into a left contact. However, it is also possible that the genuine shock may be immediately transformed into a left contact depending on the shape of the flux function (see Figures 8(b) and 8(c)). The two left contacts are merged into a genuine shock which is the final stage of the dynamics. Notice that a double sided contact never appears in this case.

6.4. Flux functions with three or more inflection points

A merging incident produces a discontinuous change of convex-concave envelops and one may add arbitrary even number of inflection points without changing the fundamental solution (see Remark 4.2(*iii*)). Therefore, only the phenomena that appear for the single or double inflection points cases are guaranteed to appear for the odd or even number of inflection points cases respectively and all the others may appear depending on the specific choice of a flux function. In Table 1, the shock types and their dynamics that can be observed from a fundamental solution are
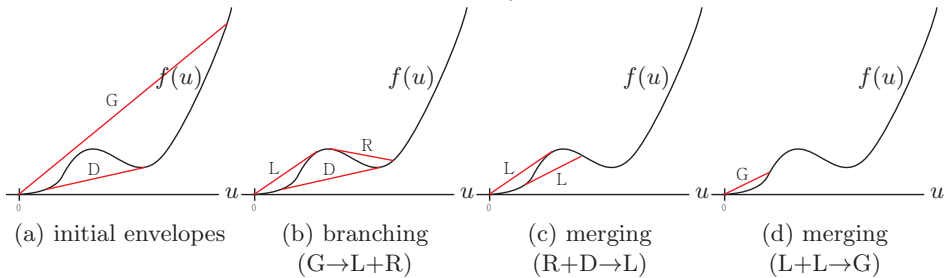
(a) initial envelopes   (b) branching   (c) merging   (d) merging
                         (G→L+R)   (R+D→L)   (L+L→G)

Figure 7. Flux function with two inflection points: Minimal model with all sorts of shocks.

(a) initial envelopes   (b) branching   (c) merging+transforming   (d) merging
                         (G→L+R)   (R+R→G→L)   (L+L→G)
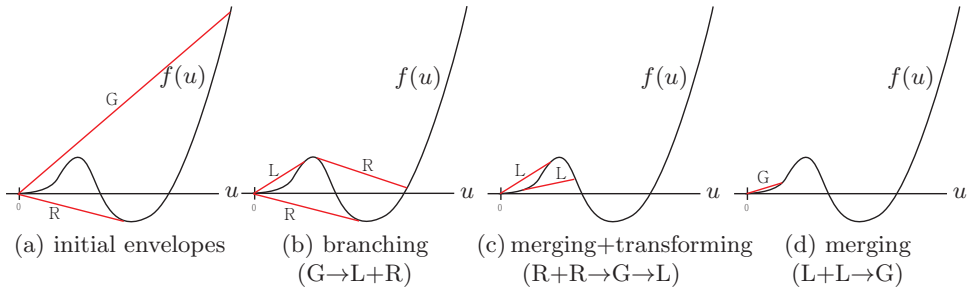
Figure 8. Flux function with two inflection points: Minimal model with all sorts of shock dynamics.

Table 1. *Some of the shock types and their dynamics may or may not appear during the evolution of the fundamental solution. This table shows which of them must or must not appear. (G,R,L and D denote genuine shock, right, left and double sided contacts, respectively. M,B and T denote merging, branching and transforming phenomena, respectively.)*

# of inflection points of flux	sign of flux	must appears	depending on flux functions	never appears
0	$f \geq 0$	G	$\emptyset$	R,L,D,M,B,T
1	$f \not\geq 0$	G,R,M,T	$\emptyset$	L,D,B
2	$f \geq 0$	G,R,L,D,M,B	$\emptyset$	T
2	$f \not\geq 0$	G,R,L,M,B,T	$\emptyset$	D
$2n-1, n \geq 2$	$f \not\geq 0$	G,R,M,T	L,D,B	$\emptyset$
$2n, \quad n \geq 2$	$f \geq 0$	G,R,L,D,M,B	$\emptyset$	T
$2n, \quad n \geq 2$	$f \not\geq 0$	G,R,L,M,B,T	D	$\emptyset$

listed with respect to the number of inflection points. In summary, one may observe only a genuine shock and a right contact if the flux function has one inflection point. However, if there are two inflection points and the flux is nonnegative, one may observe all the four types of shocks. Hence two inflection points are just enough to observe all the shock phenomena.

To justify the table, we will give examples with three and four inflection points that give all the phenomena. In this section we consider an example with three inflection points. A case with four inflection points are given in Section 7 with a discussion for a full dynamics. In Figure 9 the dynamics of the convex-concave

envelope of a flux function with three inflection points is considered. In this example

(a) initial envelopes   (b) branching (G→L+R)   (c) merging (R+D→L)

(d) merging (L+L→G)   (e) transforming (G→R)   (f) merging (R+R→G)
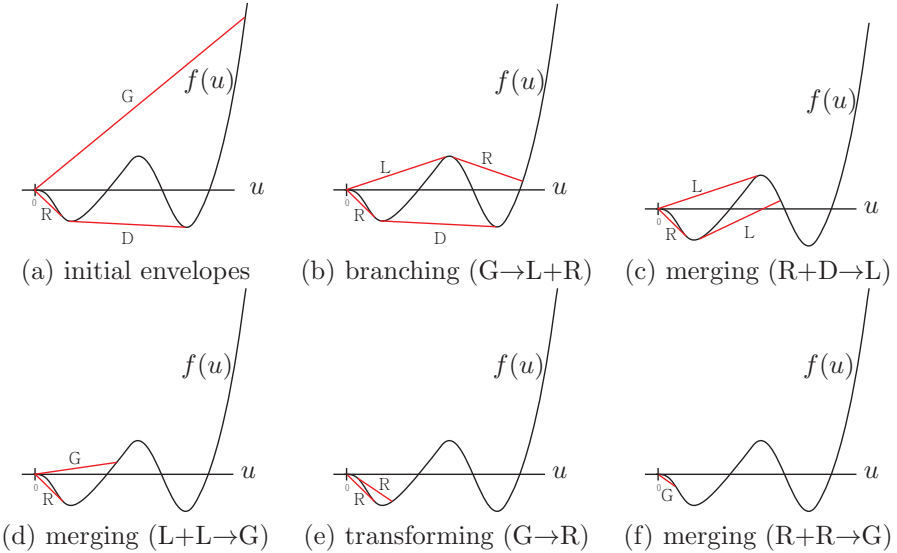
Figure 9. Flux with three inflection points: This flux gives all types of shocks and dynamics.

one may observe all the four kinds of shocks and all the three kinds of interactions. There are four merging, a single branching, and a single transforming phenomena. One may find a centered rarefaction wave fan in Figure 9(b). The final stage of the dynamics is of the genuine shock with a negative speed.

7. An example for a global picture

This section is designed to provide a complete characteristic map that shows all the dynamics of shocks and rarefaction waves discussed before. We take a flux in Figure 10 which is complicated enough for this purpose and satisfies (4.1). Since the change of an envelope is linked to each stage of a solution, all the dynamics of a solution can be interpreted in terms of envelopes. First eight figures in Figure 10 show the dynamics of the envelopes corresponding to the possible eight stages of the fundamental solution. As an example to show this connection we put an illustration of a signed fundamental solution in Figure 10(i), which belongs to the second stage, Figure 10(b). More examples of fundamental solution can be found in [13, Figures 6–8], which are actually obtained by computing the equation numerically. A complete characteristic map corresponding to this flux is given in Figure 11 with stage numbers on the left. In the rest of this section we investigate the relation between the flux and its characteristic map.

Due to the second hypothesis in (1.2), one can find a moment t_0 such that for all nonnegative $t < t_0$ the concave envelope consists of a single non-horizontal line. In the case there exists a decreasing genuine shock as denoted in Figure 10(a). In addition, there are two increasing shocks from the very beginning, a right and a double contact. These contacts are connected by a wave fan centered at the origin.
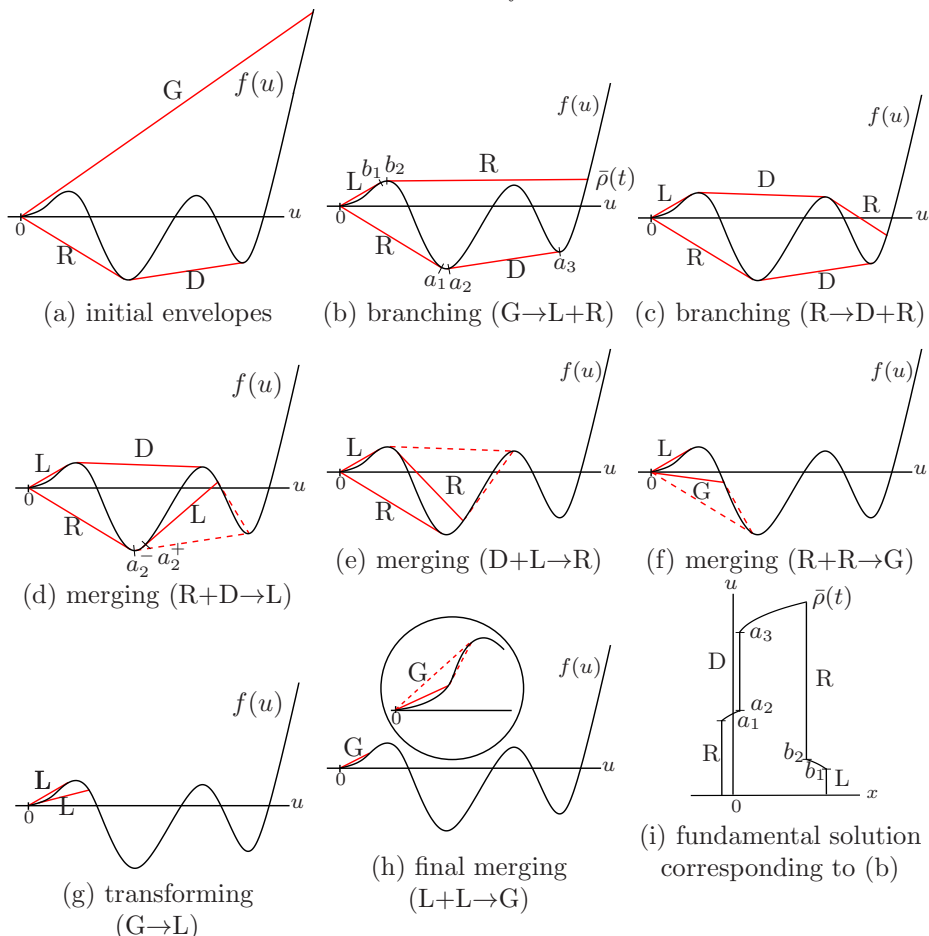
Figure 10. The envelopes of all eight stages. As the maximum of the fundamental solution decreases the corresponding envelopes change. G: genuine shock, R: right contact of single sided, L: left contact of single sided, D: contact of type D. a_j, b_j in (b), (d) for horizontal coordinates but vertical in (i).

These right and double sided contacts move with constant speeds until Figure 10(d) arrives.

The slope of the concave line corresponding to the genuine shock decreases as time t increases and hence the genuine shock curve is not a line as in Figure 11. We can observe two branching phenomena while the concave envelope moves toward 10(d), which are G→L+R in 10(b) and R→D+R in 10(c). Note that at every branching point all the curves and the line have the same slope as shown in Figure 11.

After that, we may observe three merging phenomena, D+R→L in 10(d), L+D→R 10(e), and R+R→G in 10(f). Notice that none of two contacts have the same slope after a merging phenomenon. In addition, centered wave fans appear after the first two merging phenomena. However, if a genuine shock is produced, any kind of rarefaction waves is not produced. This genuine shock moves to left slower and slower, and eventually stops. Then, the genuine shock turns into a left contact which moves
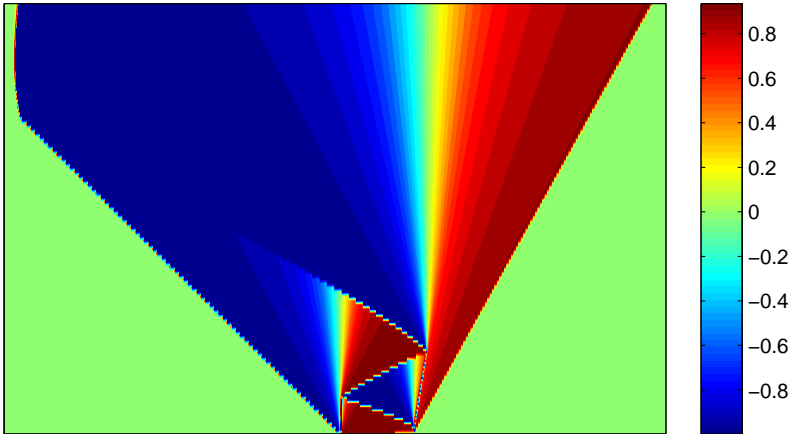
Figure 11. Dynamics of characteristics. The letter in the left indicates the stage of each strip corresponding to the stage in Figure 10.

to the right, see Figures 10(g) and 11. Note that it is possible that, after the third merging, Figure 10(f), a left contact may appear instead of the genuine shock and directly go to the stage 10(g), which is the case discussed for Figure 5(b). Finally, this left contact meets the other left contact after a long time and generates a genuine shock as in Figure 10(h). The picture in the magnified circle shows the final merging process. From this moment this genuine shock is a unique discontinuity and persists forever.

Note that Figure 11 is for an illustration purpose and made under some exaggerations to keep the whole dynamics in a single figure. It seems interesting to compare this illustration with one obtained from an actual numerical solution. In fact, we have computed a fundamental solution numerically and then displayed its dynamics in Figure 12. In the figure we have displayed up to the beginning of Figure 10(g).

The wave speed $f'(u)$ is displayed in Figure 12, where u is a numerically computed fundamental solution. One may observe the shock curves and easily distinguish if it is a left contact or a right contact. This shock curves match with Figure 11 pretty well except the ones near the initial time. For $t > 0$ small the evolution of the solution is fast and one may observe numerically if the corresponding part is magnified which is omitted here. In this figure the appearance of the centered rarefaction waves and propagation of discontinuities discussed before are more clearly observed. To produce these figures we used the WENO method. These figures in-

Figure 12. [The horizontal axis is for space x and the vertical axis is for time t.] The wave speed $f'(u)$ has been displayed in this figure. This figure clearly shows the interaction of shock waves and emerging centered rarefaction waves at the place where two shock waves are merged.

dicate that the theoretical explanation and the numerical simulation give a perfect match.

8. Discussions

Fundamental solutions are called with different names. It is called the heat kernel or the Gaussian for the heat equation, the Barenblatt solution for the porous medium equation, the diffusion wave for the Burgers equation, N-waves for the inviscid Burgers equation. There are more cases that have no specific names. For the Laplace equation case, it is simply called the fundamental solution. In all the cases the fundamental solution serves as a useful tool in understanding the behavior of solutions. If the equation is linear and autonomous, one may obtain a general solution by convoluting it with an initial value and that is why the fundamental solution is sometimes called a kernel. Even though it is not a kernel anymore in a nonlinear problem, the fundamental solution still plays a key role in theoretical development. The Oleinik one-sided inequality for convex flux is written by

$$f'(u)_x \leq 1/t, \qquad t > 0,$$

which gives the uniqueness and the sharp regularity to the conservation law. Note that the fundamental solution satisfies the equality, $f'(\rho)_x = 1/t$ and, in other words, this inequality is basically a comparison to the fundamental solution. There have been several attempts to extend the inequality to nonconvex cases (see [12, 14, 15, 21]). It is clear that the key of such an extension is in a better understanding of the fundamental solution. One may find an extension of such one-sided inequalities from the first author's recent work [18]. The asymptotic analysis is actually a study

how a solution evolves into the shape of the fundamental solution. (see, e.g., [4, 10, 16, 17]).

Notice that the solution structure discussed in this paper is only for the fundamental solution. For example Table 1 in Section 6.4 shows the shocks and their dynamics that may appear in a fundamental solution. We will briefly discuss about other cases. First, consider a Riemann problem with an initial value

$$u^0(x) = \begin{cases} u_-, & x < 0, \\ u_+, & x > 0. \end{cases}$$

If $u_- < u_+$, then the convex envelope that connects u_- and u_+ is involved and, if $u_- > u_+$, the concave envelope is involved (see [27]). Recently, Fossati and Quartapelle considered the Riemann problem for a nonconvex flux with two inflection points and applied it to systems of conservation laws (see [11]). Note that the convex and concave envelopes defined in (2.6)–(2.8) are the ones that connect the zero and the maximum of the fundamental solution. Since the maximum decreases, the convex-concave envelope evolves in time and this evolution gives the shock dynamics such as merging, branching and transforming. However, since the convex or concave envelope is fixed in a Riemann problem, such a dynamics cannot be obtain from a Riemann solver. Hence one need develop a way to recover such phenomena to use the Riemann solver to approximate a general solution.

If a piecewise constant initial value is taken, the convex and concave envelopes connecting the constant values will decide the solution dynamics until the constant part survives. If it disappears, the envelopes will be merged to make a bigger ones. The evolution of these envelopes will explain the solution dynamics. In particular, the local maximum will play the role of the maximum of the fundamental solution and one may observe various dynamics of the fundamental solution across the local maximum. One may also observe interesting phenomenon across the local minimum, which was not observed from a fundamental solution. These formal discussions need to be justified and further investigation is needed.

Note that the classification in Table 1, Section 6, depends on the technical assumption $(1.2)_2$. One may also consider the convex-concave envelopes without this assumption. For example, a Buckley-Leverett type flux function and possible envelops are given in Figure 13. This flux function has a single inflection point. One may observe a genuine shock, left contacts, and a merging phenomenon. However, other shocks types and phenomena are not observed. On the other hand, flux functions with discontinuity has been considered by many authors and one may develop a theory for such a flux function. Note that, adding a discontinuity increases the number of inflection points by two.
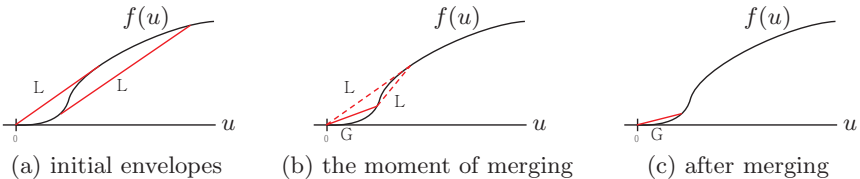

(a) initial envelopes   (b) the moment of merging   (c) after merging

Figure 13. Buckley-Leverett type flux function with a single inflection point

Acknowledgements

References

1   Donald P. Ballou, *Solutions to nonlinear hyperbolic Cauchy problems without convexity conditions*, Trans. Amer. Math. Soc. **152** (1970), 441–460 (1971). MR 0435615 (55 #8573)

2   A. L. Bertozzi, A. Münch, and M. Shearer, *Undercompressive shocks in thin film flows*, Phys. D **134** (1999), no. 4, 431–464. MR 1725916 (2001e:76042)

3   S.E. Buckley and M.C. Leverett, *Mechanism of fluid displacement in sands*, Transactions of the AIME **146** (1942), no. 1, 107–116.

4   Kuo Shung Cheng, *Asymptotic behavior of solutions of a conservation law without convexity conditions*, J. Differential Equations **40** (1981), no. 3, 343–376. MR 621249 (82h:35008)

5   ———, *Constructing solutions of a single conservation law*, J. Differential Equations **49** (1983), no. 3, 344–358. MR 715692 (84m:35074)

6   ———, *The space BV is not enough for hyperbolic conservation laws*, J. Math. Anal. Appl. **91** (1983), no. 2, 559–561. MR 690889 (84d:35096)

7   ———, *A regularity theorem for a nonconvex scalar conservation law*, J. Differential Equations **61** (1986), no. 1, 79–127. MR 818862 (88e:35121)

8   C. M. Dafermos, *Generalized characteristics and the structure of solutions of hyperbolic conservation laws*, Indiana Univ. Math. J. **26** (1977), no. 6, 1097–1119. MR 0457947 (56 #16151)

9   ———, *Regularity and large time behaviour of solutions of a conservation law without convexity*, Proc. Roy. Soc. Edinburgh Sect. A **99** (1985), no. 3-4, 201–239. MR 785530 (86j:35107)

10   Jean Dolbeault and Miguel Escobedo, L^1 *and* L^∞ *intermediate asymptotics for scalar conservation laws*, Asymptot. Anal. **41** (2005), no. 3-4, 189–213. MR 2127996 (2006i:35233)

11   Marco Fossati and Luigi Quartapelle, *The Riemann problem for hyperbolic equations under a nonconvex flux with two inflection points*, arXiv:1402.5906 [physics.flu-dyn].

12   Olivier Glass, *An extension of Oleinik's inequality for general 1D scalar conservation laws*, J. Hyperbolic Differ. Equ. **5** (2008), no. 1, 113–165. MR 2405854 (2009c:35292)

13   Youngsoo Ha and Yong-Jung Kim, *The fundamental solution of a conservation law without convexity*, Quart. Appl. Math. (to appear).

14   David Hoff, *The sharp form of Oleĭnik's entropy condition in several space variables*, Trans. Amer. Math. Soc. **276** (1983), no. 2, 707–714. MR 688972 (84b:35080)

15   Helge Kristian Jenssen and Carlo Sinestrari, *On the spreading of characteristics for nonconvex conservation laws*, Proc. Roy. Soc. Edinburgh Sect. A **131** (2001), no. 4, 909–925. MR 1855004 (2002h:35179)

16   Yong-Jung Kim, *Asymptotic behavior of solutions to scalar conservation laws and optimal convergence orders to N-waves*, J. Differential Equations **192** (2003), no. 1, 202–224. MR 1987091 (2004e:35147)

17   ———, *Potential comparison and asymptotics in scalar conservation laws without convexity*, J. Differential Equations **244** (2008), no. 1, 40–51. MR 2373653 (2009d:35220)

18   ———, *A geometric one-sided inequality for zero-viscosity limits*, preprint, http://arxiv.org/abs/1306.3577 (2013).

19   S. N. Kružkov, *First order quasilinear equations with several independent variables.*, Mat. Sb. (N.S.) **81 (123)** (1970), 228–255. MR 0267257 (42 #2159)

20   P. D. Lax, *Hyperbolic systems of conservation laws. II*, Comm. Pure Appl. Math. **10** (1957), 537–566. MR 0093653 (20 #176)

21   Philippe G. Lefloch and Konstantina Trivisa, *Continuous Glimm-type functionals and spreading of rarefaction waves*, Commun. Math. Sci. **2** (2004), no. 2, 213–236. MR 2119939 (2005i:35174)

22 Tai Ping Liu, *Admissible solutions of hyperbolic conservation laws*, Mem. Amer. Math. Soc. **30** (1981), no. 240, iv+78. MR 603391 (82i:35116)

23 Tai-Ping Liu and Michel Pierre, *Source-solutions and asymptotic behavior in conservation laws*, J. Differential Equations **51** (1984), no. 3, 419–441. MR 735207 (85i:35094)

24 O. A. Oleĭnik, *Discontinuous solutions of non-linear differential equations*, Uspehi Mat. Nauk (N.S.) **12** (1957), no. 3(75), 3–73. MR 0094541 (20 #1055)

25 Tao Tang, Zhen-Huan Teng, and Zhouping Xin, *Fractional rate of convergence for viscous approximation to nonconvex conservation laws*, SIAM J. Math. Anal. **35** (2003), no. 1, 98–122. MR 2001466 (2004i:35221)

26 A. I. Vol′pert, *Spaces* BV *and quasilinear equations*, Mat. Sb. (N.S.) **73 (115)** (1967), 255–302. MR 0216338 (35 #7172)

27 Burton Wendroff, *The Riemann problem for materials with nonconvex equations of state. I. Isentropic flow*, J. Math. Anal. Appl. **38** (1972), 454–466. MR 0328387 (48 #6729)